



1 **Vegetation and fire anomalies during the last ~70 ka in the Ili Basin, Central Asia, and their**
2 **implications for the ecology change caused by human activities**

3
4 **Yunfa Miao^{a, b*}, Yougui Song^{b, c*}, Yue Li^{b, d}, Shengli Yang^e, Yun Li^b**

5
6 a. Key Laboratory of Desert and Desertification, Northwest Institute of Eco-Environment and
7 Resources, Chinese Academy of Sciences, Lanzhou 730000, China

8 b. State Key Laboratory of Loess and Quaternary Geology, Institute of Earth Environment,
9 Chinese Academy of Sciences, Xi'an 710061, China

10 c. Research Center for Ecology and Environment of Central Asia, Chinese Academy of Sciences,
11 Urumqi, 830011, China

12 d. College of Resources and Environment, University of Chinese Academy of Sciences, Beijing,
13 100049 China

14 e. Key Laboratory of Western China's Environmental Systems (Ministry of Education), College of
15 Earth and Environmental Sciences, Lanzhou University, Lanzhou, 730000, China

16 Corresponding author: miaoyunfa@lzb.ac.cn; ygsong@loess.llqg.ac.cn

17
18 **Abstract:** Changes in vegetation characteristics and fire occurrence during the last glacial period
19 offer an opportunity to better understand paleoclimate change and past human activities as well as
20 the relationships among them. However, in central Asia, records of both vegetation and fire have
21 rarely been obtained from the same profile. Here, for the first time, we present pollen and
22 microcharcoal data collected together from the wind-blown loess Nileke section, representing the
23 past ~70 thousand years (ka) in the Ili Basin, Northwest China, Central Asia. These records enable
24 investigation of the pollen-based vegetation and microcharcoal-based fire proxies as well as their
25 possible relationships with ancient human activities. The results show that the temperate
26 herbaceous taxa remained at relatively low levels before 36 ka, whereas the temperate woody taxa,
27 especially Cupressaceae, were abundant. At the same time, the fire frequencies were relatively low.
28 After 36 ka, herbaceous taxa abruptly replaced Cupressaceae and the fire occurrence gradually
29 increased. We named this change as the local vegetation degeneration event, because no
30 equivalent changes have been identified anywhere else across Eurasia. Prior to the event, a period



31 of intensified fire activity occurred between 47.5 and 36 ka, although the background fire activity
32 was relatively low. We argue that the intensified local fire activity was the primary factor causing
33 the vegetation event and was mainly driven by human activity. Following migrations from Africa
34 after 200 ka, humans began to colonize the Ili Basin at least 47.5 ka ago, bringing their skills of
35 fire control and consequential destruction of woody vegetation. Future analysis of first-hand
36 archeological sites in this area will be an important step in supporting our hypothesis.

37

38 **Keywords:** Vegetation; Fire; Ecology; Human activities; Last glacial period

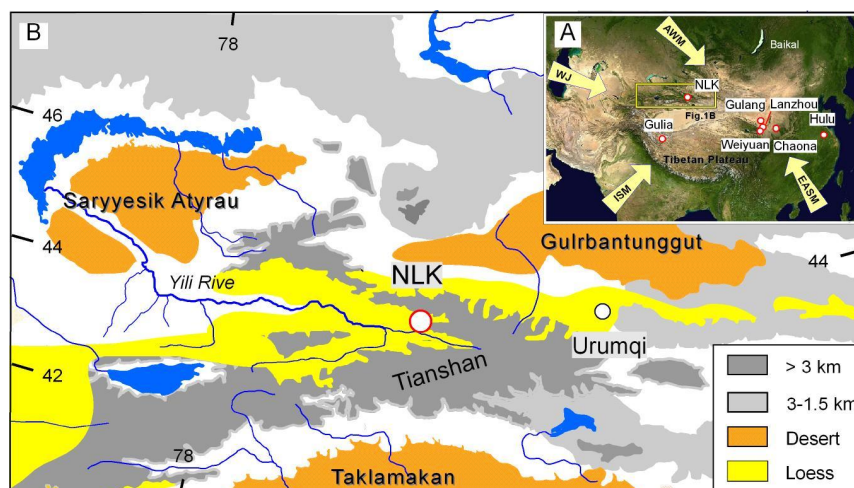
39

40 **1. Introduction**

41 The climate, vegetation, fire and human activities, as well as the relationships among them
42 over the late Quaternary, especially the last glacial period, provide basic insights by which to
43 understand the future (e. g., Behling and Safford, 2010; Cheng et al., 2012; Li et al., 2013; Hubau
44 et al., 2015; Varela et al., 2015). High-resolution stalagmite (Wang et al., 2001; Cheng et al., 2016),
45 ice core (Thompson et al., 1997; Petit et al., 1999; Augustin et al., 2004) and loess (e.g., Chen et
46 al., 1997; Hao et al., 2012; Sun et al., 2012) analysis has yielded highly reliable, integrated
47 paleoclimate records. These are characterized by a series of strong fluctuations, named cold
48 Heinrich or warm Dansgaard-Oeschger events, as well as a warm middle Holocene (e.g., Bond et
49 al., 1997). At the eastern margin of Central Asia, precipitation has followed the same patterns as
50 these events: lower precipitation during the cold events and vice versa (e.g., Rao et al., 2013).
51 Vegetation is regarded as one of the most sensitive proxies for climate change, and a limited
52 number of complete vegetation records have been obtained to show how the terrestrial ecological
53 landscape responded to climate change (e.g., Guiot et al., 1993; Allen et al., 1999; Jiang et al.,
54 2011). Fire is another sensitive proxy used for reconstructing climate (e.g., Filion, 1984; Bird and
55 Cali, 1998; Bowman et al., 2009). Besides climate, records of vegetation and fire are also unique
56 indicators of human activities, owing to the impact of human activities such as vegetation cutting
57 and burning (e.g., Patterson et al., 1987; Whitlock and Larsen, 2002; Huang et al., 2006; Aranbarri
58 et al., 2014; Miao et al., 2016b; Sirocko et al., 2016); however, most relevant studies have been
59 limited to the late Holocene, especially at archeological sites. Few studies have attempted to
60 reconstruct the last glacial period, despite this period being considered as a key period of



61 migration: the human migration from Africa started at around 200 ka (Templeton, 2002; Sun et al.,
62 2012). Furthermore, studies of vegetation and fire within the same profile (section or core) are
63 helpful in understanding the vegetation, fire and climate, as well as human activities (e.g., Zhao et
64 al., 2010; Xiao et al., 2013; Miao et al., 2016a; b).



65
66 *Figure 1. A. Asian morphological map with climate systems showing the NLK (Nileke) section*
67 *location and climatic proxy sites covering the past 70 ka. These sites include the Gulia glacial*
68 *core (Thompson et al., 1997), Gulang wind-blown sediments (Sun et al., 2012), Chaona (Wang et*
69 *al., 2016), Hulu stalagmite oxygen isotope records (Wang et al., 2001), Weiyuan summer*
70 *precipitation reconstruction (Rao et al., 2013) and Lanzhou pollen analysis (Jiang et al., 2011). B.*
71 *A morphological map showing the location of the Nileke section in this study.*

72

73 Central Asia is dominated by a dry climate (Figure 1A), which is very sensitive to any
74 climate changes (fluctuations or abnormality) and human activities. In this study, we firstly
75 present pollen and microcharcoal results from a wind-blown loess sediment section (Figure 1B) to
76 reveal how vegetation and fire activity have changed during the past 70 ka; we then analyze the
77 mechanisms underlying these changes.

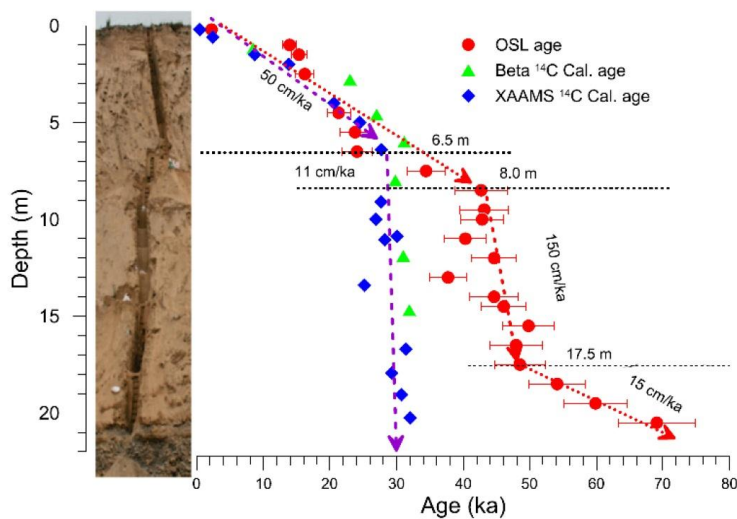
78 2. Materials and methods

79 2.1 Lithostratigraphy and chronology

80 The Ili Basin is surrounded by the Tianshan orogenic belt in east Central Asia, with gentle
81 topography to the west. The basin opens to the west and funnels winds and cyclonic disturbances,



82 often associated with prevailing westerly winds, down its axis (Ye, 2001). The Ili Basin has a
83 temperate, continental, arid climate with a mean annual temperature that varies from 2.6 °C at
84 1850 m to 10.4 °C at 660 m; the mean annual precipitation varies correspondingly from 512 to 257
85 mm (Ye et al., 1997; Ye, 2001). The surface soils are a sierozem (aridosols) with widely
86 distributed desert steppe vegetation. The vegetation coverage is <50%, mainly comprising
87 *Artemisia* spp. and *Chenopodiaceae* spp. (Ye et al., 2000). There are no obvious accumulations of
88 organic matter in the surface horizon of the modern soil.



89
90 *Figure 2. Stratigraphy and dating for the Nilke Section (for more detail see Song et al. 2015).*

91
92 To the west of the Ili Basin are the vast central Asian Gobi Deserts, such as Saryesik-Atyrau
93 Desert (Figure 1B), the probable source of dust for Late Pleistocene loess deposits. The loess
94 deposits are widely distributed across the piedmont of the Tianshan Mountains, river terraces and
95 desert margins. The loess thickness ranges from several meters to approximately two hundred
96 meters, and there are two primary depocenters: around Sangongxiang in the northwest and
97 Xinyuan in the east Ili basin (Song et al., 2014). Most of the loess appears to have been deposited
98 since the last interglacial period (ca. 130 ka; Ye, 2001; Song et al., 2010; 2014; Li et al., 2016).

99 The Nileke section (83.25 °E, 43.76 °N, 1253 m a. s. l) is located on the second terrace of the
100 Kashi River, a branch of the Ili River, in the east Ili Basin (Figure 1B). The loess sequence is 20.5



101 m thick, largely homogeneous in appearance with two diffuse paleosols at depths of 5-7.5 m and
102 15.5-18.5 m identified by the extent of rubification (Figure 2) (Song et al., 2015). The loess
103 sequence rests conformably on fluvial sand and gravels. The contact between the loess and fluvial
104 sediment is abrupt with no obvious lag, erosion or pedogenesis. The loess is composed of 70%-84%
105 silt and 3%-17% very fine sand (63-100 μm), with the remaining fraction being clay. A
106 high-resolution quartz optically stimulated luminescence (OSL) chronology has already been
107 established (Yang et al., 2014; Song et al., 2015). Based on OSL ages, two intervals of higher mass
108 accumulation rate occurred at 49-43 ka and 24-14 ka (Song et al., 2015).

109 2.2 Pollen and charcoal collection

110 A total of 104 samples of 49-56 g weight were taken at 20 cm intervals from the Nileke
111 section for palynological analysis. The samples were treated with standard palynological methods:
112 acid digestion (treatment with 10% HCl and 40% HF acid to remove carbonates and silicates,
113 respectively) (Li et al., 1995) and fine sieving to enrich the spores and pollen grains. The prepared
114 specimens were mounted in glycerol for identification. All samples were studied at the Cold and
115 Arid Regions Environmental and Engineering Research Institute (CAREERI), Chinese Academy
116 of Sciences (CAS), by comparison with official published pollen plates and modern pollen
117 references. Each pollen sample was counted under a light microscope at 400× magnification in
118 regularly spaced traverses. More than 150 spores and pollen grains were counted within each
119 sample. A known number of *Lycopodium clavatum* spores (batch # 27600) were initially added to
120 each sample for calculation of pollen and microcharcoal concentrations (Maher, 1981).

121 The concentration of pollen or microcharcoals can be calculated according to the following
122 formula: $C=N_x/L_x \times 27600/W_x$

123 C: concentration; N: identified number of charcoals; L: number of *Lycopodium clavatum*; W:
124 sample dry weight; x: sample number; 27600: grain numbers of *Lycopodium clavatum* per pill.

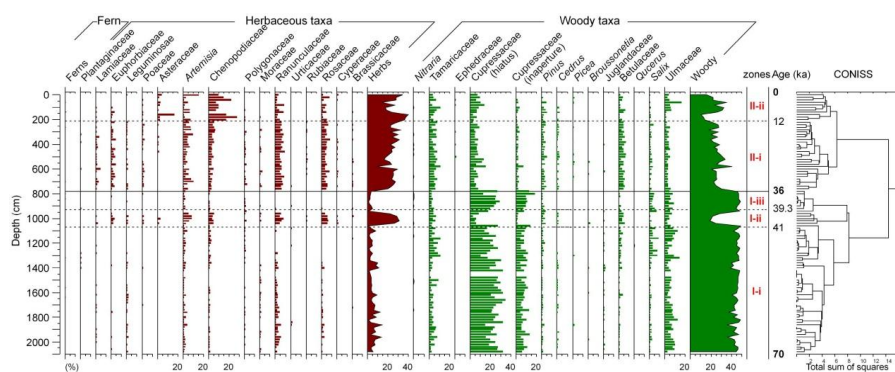
125 For the microcharcoal identification, four particle size units were defined as follows: <30 μm,
126 30-50 μm, 50-100 μm and >100 μm (Miao et al., 2016a), then the total microcharcoal
127 concentrations (MC) were obtained by summing over all sizes and using the above formula. As
128 the residual matter from the incomplete burning of vegetation, charcoals are usually characterized
129 by either spherical bodies without structure or particles with some original plant structures
130 preserved.



131 3. Results and analysis

132 In the pollen assemblages, dominant palynomorphs originated mainly from herbaceous taxa
133 such as Chenopodiaceae, *Artemisia*, Ranunculaceae, Asteraceae and Rosaceae. Woody taxa were
134 Cupressaceae, *Pinus*, *Betula*, Ulmaceae and Tamaricaceae; the other temperate taxa with low
135 percentages were *Quercus*, *Picea*, *Cedrus* and *Broussonetia* etc.

136



137

138

Figure 3. Pollen percentage diagram for the Nileke section, Ili Basin.

139

140 The pollen diagram was divided into two pollen assemblage zones based on variations in the
141 percentages according to stratigraphically-constrained cluster analysis (CONISS) carried out using
142 Tilia software (E. Grimm of Illinois State Museum, Springfield, Illinois, USA) (Figure 3) and
143 concentrations of the dominant taxa, from the older to the younger samples. The two zones are as
144 follows.

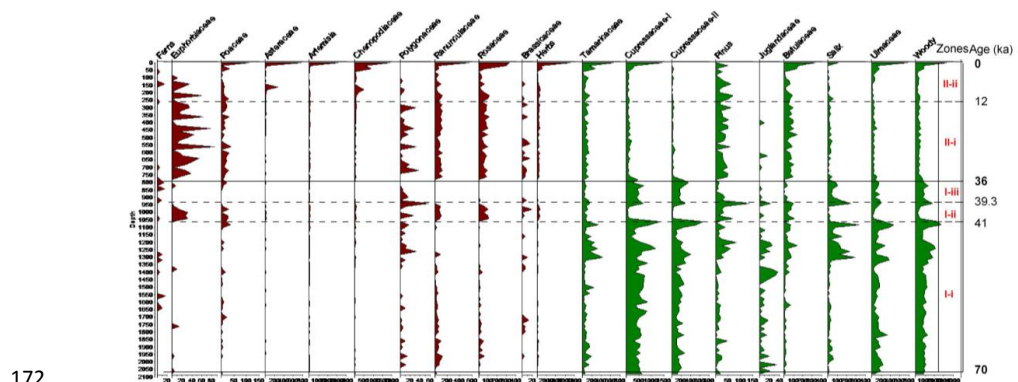
145 Zone I (2080-780 cm; 70-36 ka): the assemblages were characterized by high percentages of
146 Cupressaceae (hiatus) (ca. 5.2%-68.7%, with an average of 42.4%) and Cupressaceae (inaperture)
147 (ca. 1.4%-34.7%, average 14.0%), Ulmaceae (ca. 2.8%-26.1%, average 11.3%), Tamaricaceae (ca.
148 1.9%-20.9%, average 7.3%). In the herbaceous taxa, only *Artemisia* (ca. 0-14.8%, average 3.3%),
149 Ranunculaceae (ca. 0-14.2%, average 3.0%) and Chenopodiaceae (ca. 0-8%, average 1.8%) were
150 dominant, and at much lower abundances relative to the woody taxa. In more detail, three
151 subzones were identified according to the assemblages: I-i, I-ii and I-iii with divisions at 1070 and
152 930 cm, corresponding to ages of 41 ka and 39.3 ka. The subzones I-i and I-iii were both
153 characterized by high Cupressaceae, whereas subzone I-ii was relatively dominated by herbaceous



154 taxa.

155 In the pollen concentrations, the same zones were also identified at a depth of 780 cm. The
156 woody taxa were dominant below this boundary, and those such as Cupressaceae (hiatus and
157 inaperture), Ulmaceae and Tamaricaceae reached counts of around 1000 grains/g, 200 grains/g
158 and 100 gains/g respectively. Others such as *Pinus*, Juglandaceae, *Betula* and *Salix* were also
159 common. By contrast, all herbaceous taxa were very low (Figure 4). We also added the boundary
160 at a depth of 780 cm to divide the MC assemblages. Below the boundary, the fluctuations in all
161 different sizes and shapes were stronger, especially in Zones I-ii and I-iii (Figure 5).

162 Zone II (780-0 cm; 36-0 ka): the woody taxa were extensively replaced by herbaceous taxa,
163 of which Cupressaceae (hiatus) (ca. 3.5%-51.0%, average 12.1%) and Cupressaceae (inaperture)
164 (ca. 0-24.5%, average 2.9%), Tamaricaceae (ca. 1.5%-19.4%, average 8.9%) and Ulmaceae (ca.
165 0.5%-27.9%, average 5.6%) were dominant; *Betula* and *Pinus* increased slightly (ca. 0-12.6%,
166 average 6.4% and ca. 0-8.6%, average 2.3%, respectively). In the herbaceous taxa, *Artemisia* (ca.
167 0.9-24.1%, average 7.1%), Chenopodiaceae (ca. 0-48.2%, average 9.0%), Rosaceae (ca. 0-15.0%,
168 average 8.6%) and Rannunculaceae (ca. 0-14.2%, average 3.0%) increased obviously, and the rest
169 remained broadly stable. In more detail, two sub-horizons were identified: II-i and II-ii, divided
170 based on the Asteraceae and Chenopodiaceae increase at 210 cm, correlated to an age of 12 ka B.P.
171 (Figure 3).



172
173 Figure 4. Pollen concentration diagram for the Nileke section, Ili Basin, China (zone divisions
174 follow Figure 3).

175

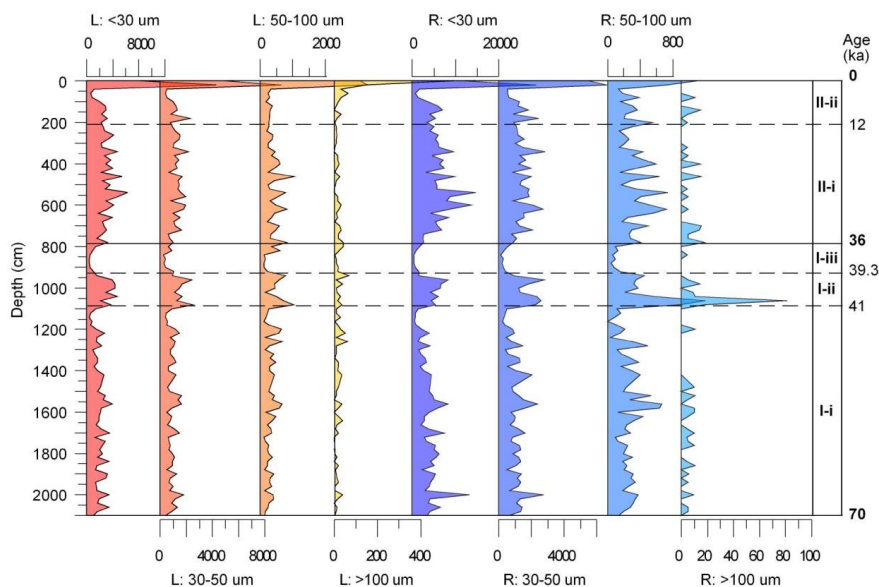
176 The pollen concentrations in Zone II show that the woody Cupressaceae (hiatus and



177 inaperture), Ulmaceae, Juglandaceae and Tamaricaceae decreased obviously while the herbaceous
178 taxa such as *Artemisia*, Chenopodiaceae, Poaceae, Ranunculaceae and Rosaceae increased. At the
179 sub-boundary of II-i and II-ii, Asteracea, *Artemisia* and Chenopodiaceae increased strongly
180 (Figure 4). For the MC, all different shapes and sizes remained at generally stable and relatively
181 low values in Zone II-i whereas in Zone II-ii the concentrations in all samples clearly started to
182 increase, especially in the uppermost layers (Figure 5).

183 In summary, there are clear divisions at a depth of 780 cm, corresponding to an age of 36 ka.
184 Prior to this change there was a high percentage of woody taxa, but subsequently the herbaceous
185 taxa became more dominant, especially after 12 ka. The assemblages of pollen concentrations and
186 MC can also be divided into two periods, with a transition at 36 ka.

187



188

189 Figure 5. The MC records for different sizes and shapes in the Nileke section (unit: grains/g; L:
190 elongated; R: zone divisions follow Figure 3).

191

192 4. Discussion

193 The modern climate in Central Asia is controlled by the East Asian summer monsoon, Indian
194 summer monsoon, Asian winter monsoon and Westerlies (Figure 1A). In the Ili Basin,
195 meteorological records indicate that strong surface winds from the west, northwest and southwest



196 which occur frequently from April to July play the dominant role in the transportation of dust,
197 suggesting that the wind-blown sediments in the Nileke section are driven by the Westerlies.
198 Therefore, the grain size of the sediments can be regarded as a basic proxy for the intensification
199 of the Westerlies (Li et al., 2015; Li et al., 2016). Furthermore, the Ili Basin is surrounded by the
200 Tianshan Mountains to the south, east and north (with elevations exceeding 3-4 km) but low
201 elevations (~800-1600 m a. s. l) to the west. Consequently, most of the precipitation reaching the
202 basin will have been transported by the Westerlies during the last glacial period. Here, we try
203 firstly to estimate changes in the vegetation and fire characteristics in the Ili Basin, secondly to
204 discuss the overall climate change across Eurasia over the past 70 ka, and finally provide some
205 speculation regarding the differences.

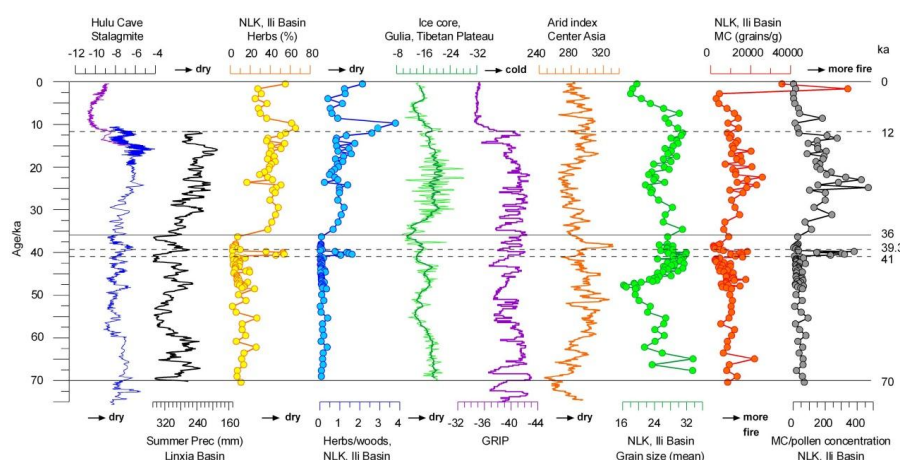
206 **4.1 Vegetation and fire records at Nileke**

207 The pollen dataset can be regarded as a reliable proxy for investigating the vegetation change
208 in the study area. In the Nileke section, during 70-36 ka, the pollen assemblages show a relatively
209 woody taxa-dominated landscape: during this time, the woody taxa reached their highest levels of
210 the whole section (Figure 6). After 36 ka, the vegetation deteriorated markedly, as evidenced by
211 the rapid disappearance of woody taxa following strong fluctuations during 41-36 ka. This was
212 especially notable for Cupressaceae. In more detail, no obvious fluctuations were noted during
213 these two periods except for the interval between 41 and 36 ka. The pollen concentrations also
214 follow a similar trend, according to the pollen percentages. Overall, the most obvious vegetation
215 change according to the pollen data was at around 36 ka ago, as indicated by the sharp change in
216 vegetation assemblages. A similar transition has not been observed in Europe (e.g., Guiot et al.,
217 1993; Allen et al., 1999) or elsewhere in Asia (e.g., Jiang et al., 2011).

218 Charcoal particles remaining following combustion are entrained by the smoke and then
219 carried by the wind. Following deposition, they remain as a direct proxy of fire activity. On the
220 Loess Plateau, smaller charcoal particles can be easily transported over long distances by the wind,
221 but the larger particles tend to travel only a short distance (Huang et al., 2006). Therefore, the
222 charcoal particle size can be related to its distance from the fire (Patterson et al., 1987; Clark, 1988;
223 Luo et al., 2006; Miao et al., 2016a; b), with smaller particles likely to have been transported
224 further from the fire (Clark, 1988). Moreover, a rounder shape (long axis to short axis ratio <2.5)
225 is more likely related to forest fires while elongated particles (long axis to short axis ratio >2.5)



226 are more indicative of grass fires (Umbanhowar and Mcgrath, 1998; Crawford and Belcher, 2014).
 227 The charcoal assemblages in the Ili Basin show a relative low fire frequency/severity at regional
 228 and local scales, in forest and grass, before 36 ka; activities then increased gradually after 36 ka
 229 (Figure 6, 7). Superimposed on this general trend, the first notable anomaly occurred at 47.5-36 ka
 230 and was characterized by a high frequency of local grass and forest fires. Another similar anomaly
 231 occurred at the top of the profile (less than 6 ka) in the layer with the highest levels of regional and
 232 local grass fires as well as the highest regional forest fires (Figure 3-5).



233
 234 *Figure 6. Comparison of climate proxies across the Northern Hemisphere and Nile section.*
 235 *These are Hulu cave, Nanjing (Wang et al., 2001); summer precipitation reconstruction in the*
 236 *Linxia Basin (Rao et al., 2013); ice core, Gulia, Tibetan Plateau (Thompson et al., 1997); NGRIP*
 237 *(Andersen et al., 2004); and aridity index in central Asia (Li et al., 2013). Divisions follow Fig. 3.*
 238 *No anomalies occurred during 41-36 ka.*

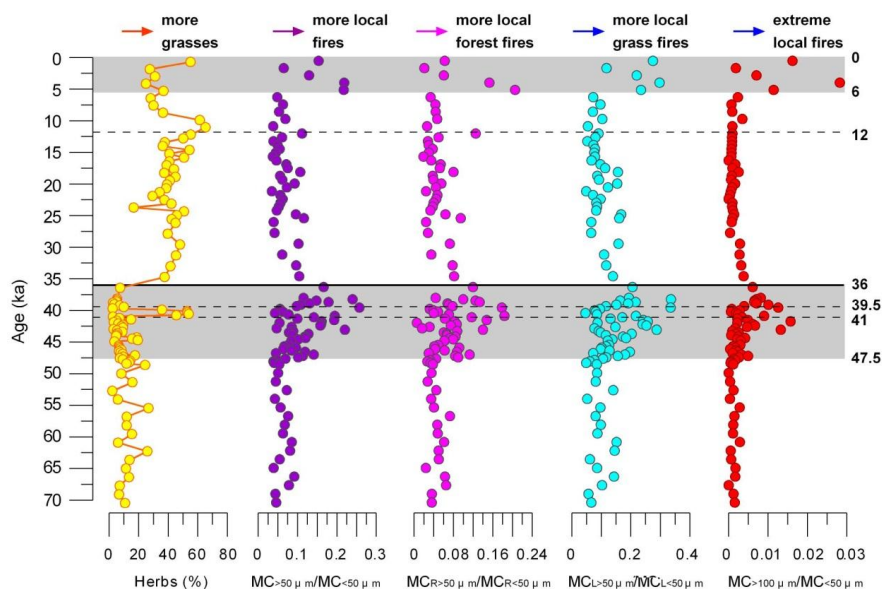
239

240 4.2 Climate in Eurasia

241 Here, multiple proxies from the terrestrial and marine sources have revealed the basic patterns
 242 of climate change during the last glacial period, characterized by abrupt, millennial-scale cold
 243 events (Petit et al., 1999; Wang et al., 2001; Augustin et al., 2004; Cheng et al., 2016) (Figure 6).
 244 These climate fluctuations are particularly pronounced in records of the East Asian monsoon
 245 system (Porter and An, 1995; Guo et al., 1996; Thompson et al., 1997; Wang et al., 2001; Sun et
 246 al., 2012).



247 The Greenland NGRIP ice core (Andersen et al., 2004) indicates that temperature variations
 248 in the high latitudes of the Northern Hemisphere are characterized by high-frequency fluctuations
 249 over the past 70 ka, with the most obvious change occurring at around 12 ka and no significant
 250 anomaly at 36 ka. At the same time, high-resolution summer precipitation variations in the
 251 western Chinese Loess Plateau were found to contain similar anomalies (Rao et al., 2013), yet
 252 with no obvious precipitation change at around 36 ka, despite their proximity to the Lanzhou loess
 253 sediments, where the shrubs and herbs reached the highest abundances after ~40 ka owing to the
 254 westerlies strengthening and supplying plenty of moisture to Northwest China (Jiang et al., 2011).
 255 In Europe the newest study shows that during 49-36.5 ka, the boreal forest of pine, birch and few
 256 spruce with little dust activity, however the charcoal indicates drought stress and frequent forest
 257 fires. During 36.5-28.5 ka, the steppe with grass, pine and birch enlarged. Dust storm increased.
 258 Spread of anatomically modern humans in the increasingly open landscape, where horse, reindeer
 259 and mammoth, the favored hunting preys, must have been abundant (Sirocko et al., 2016). This
 260 time is correlated with the time of early modern humans spreading into central Europe (Trinkaus
 261 et al., 2003; Mellars, 2006; Conard and Bolus, 2008; Klein, 2008; Hublin, 2012; Nigst et al.,
 262 2014).



263
 264 *Figure 7. Vegetation versus fire anomalies identified in the Nileke section during 47.5-36 kyr.*
 265 *Gray rectangles show periods of intensified local fire activity during 47.5-36 and 6-0 kyr, which*



266 *cannot be explained as the result of the climate change.*

267

268 Therefore, we argue that the natural climate change at around 36 ka is not the main cause for
269 the vegetation changes in the Ili Basin. Furthermore, the aridity index in Central Asia reveals that
270 the change at ~36 ka did not shift the climate away from its generally arid classification (Li et al.,
271 2013). Another potential factor to consider is the wind velocity change, however according to the
272 grain-size distribution of the sediments in the Nileke section, there was no obvious change in the
273 mean size and accordingly no significant variation in wind during that time (Figure 6).

274 **4.3 Climate and fire anomalies and their driving forces**

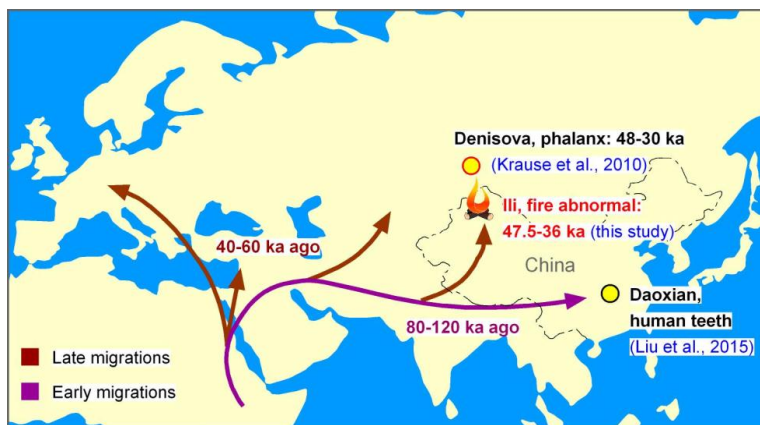
275 According to the oxygen isotope records from Greenland (Andersen et al., 2004) and Hulu
276 Cave (Wang et al., 2001), as well as data from summer precipitation (Rao et al., 2013) and the
277 aridity index established for Central Asia (Sun et al., 2012), the climate across Central Asia has
278 maintained steady large-scale patterns with no substantial changes since 36 ka. Levels of CH₄
279 (Blunier and Brook, 2001) and CO₂ (Ahn and Brook, 2008) during this period remained within the
280 bounds of normal fluctuations. So, large-scale climate change across Eurasia cannot be the
281 primary factor explaining vegetation anomalies in the Ili Basin.

282 Excluding climate change, fire can be another factor causing changes to vegetation and land
283 cover (Miao et al., 2016a), with potential for then causing a climate anomaly. In Figure 7, we
284 compiled the microcharcoal data to investigate the fire intensity on a relatively regional scale
285 ($MC_{>50 \mu m}/MC_{>50 \mu m}$), including local forest fire ($MC_{R>50 \mu m}/MC_{R>50 \mu m}$) and local grass fire
286 ($MC_{L>50 \mu m}/MC_{L>50 \mu m}$) as well as extreme local fire events ($MC_{>100 \mu m}/MC_{<50 \mu m}$), according to the
287 different shapes and sizes (see section 4.1). The results revealed two obvious fire anomaly periods:
288 one during 47.5-36 ka, when local and extreme-local fires were markedly more intense, with a
289 sharp decrease at 36 ka; the second was during 6-0 ka, again characterized by strong local and
290 extreme-local fires.

291 In nature, wildfire has existed since the vegetation began to colonize the land (Glasspool et
292 al., 2004). According to Holocene fire records from the Northeast Tibetan Plateau (Miao et al.,
293 2016b), as well as global records on orbital time scales (Bird and Cali, 1998; Luo et al., 2001), the
294 climate change might have strongly driven the fire changes by changing humidity. Summer
295 precipitation during 41-36 ka was at its highest level of the past 70 ka (Rao et al., 2013), which



296 will have impeded burning. So, the precipitation change was not the key factor in the observed fire
297 anomalies. Another possibility is that the fire was caused by human activities. The earliest
298 human-controlled fire can be traced back to at least 0.8 million years in Israel (Goren-Inbar et al.,
299 2004) or 0.4-0.5 million years for *Homo erectus pekinensis* in China (Weiner et al., 1998), which
300 means that after that the humans have colonized the worldwide regions in the latest period of the
301 Pleistocene e.g., the last glacial period with the skills of fire control. The Ili Basin, as one of most
302 important passageways from Africa to high-latitude of Asia, e.g., Baikal Lake, can be burned
303 during their colonization, thus the natural vegetation during their colonization should have been
304 changed or destroyed strongly, especially including the arbors. Cupressaceae as one sensitive
305 woody species in the mid latitude of Inner Asia grow slowly and, once destroyed, regrowth is very
306 slow. This could explain why Cupressaceae disappeared so fast following human colonization.



307
308 *Figure 8. An early migration from Africa (adapted from Callaway, 2015). Finds in the Ili Basin dated*
309 *to 47.5-36 kyr correlate with human fire activity (this study).*

310
311

312 There is widespread evidence supporting human occupation of Central Asia during the
313 Holocene (Huang et al., 1988; Wang and Zhang, 1988; Taklimakan Desert archaeology group,
314 1990; Yidilis, 1993; Lü et al., 2010; Zhang et al., 2011; Tang et al., 2013; Han et al., 2014). In the
315 Ili Basin, although direct archeological sites are limited, the coeval local fire intensification
316 supports human activity as a factor causing fire anomalies after around 6 ka. This relationship can
317 be similarly extended to observed fire anomalies at 47.5-36 ka, when humans migrated into the Ili



318 Basin. Although direct archeological proofs of fire usage at this time are still lacking, human
319 colonization of mid-to high-latitude Eurasia occurred after 200 to 80 ka (Wu et al., 2015) and
320 extended to Central Asia after around 60-40 ka (Callaway, 2015), for example, In Denisova Cave,
321 the Altai Mountains, Russia. The phalanx was found in a stratum dated to 48–30 ka ago (Krause et
322 al., 2010) (Figure 8). So, it is not difficult to link the local fire anomalies during 47.5-36 ka in the
323 Ili Basin to human activities: the increased occurrence of local fires (for cooking, or burning the
324 uncultivated land) quickly destroyed the vegetation, causing the observed vegetation degeneration.
325 If this is the case, the modern vegetation may have originated since around 36 ka. In future the use
326 of a massive and sustained ecological program of vegetation rehabilitation in the arid and semiarid
327 region should reduce the risk of destructive fire in order to avoid a similar local vegetation disaster
328 to that which occurred at 36 ka.

329

330 **5. Conclusions**

331 In the Nileke Section, Ili Basin, the pollen assemblages show a sharp change at ~36 ka
332 characterized by herb increase and Cupressaceae decrease, which is difficult to be explained in
333 terms of a Eurasian climate anomaly and instead is attributed to local vegetation degradation
334 caused by local fire intensification. Human activities during 45-36 ka are inferred as the main
335 driving force of this change, although direct archeological proofs are still lacking. In future, new
336 archeological sites in this area are required to investigate the extent to which ancient human
337 activities influenced the vegetation. This will provide further insights into the relationships
338 between human fire activity and local vegetation and even climate change.

339

340 **Acknowledgements**

341 The project is supported by the Natural Science Foundation of China (Nos: 41572162,
342 41472147 and 41271215), the National Key Research and Development Program of China (Nos:
343 2016YFA0601902), International partnership Program of Chinese Academy of Science (grant
344 number: 132B61KYS20160002), and the State Key Laboratory of Loess and Quaternary Geology,
345 Institute of Earth Environment, CAS (SKLLQG1515) and Open Foundation of MOE Key
346 Laboratory of Western China's Environmental System, Lanzhou University (lzujbky-2015- bt01).
347 The authors thank Y. Li, X. Li, J. Dong and F. Zhang for sampling and laboratory assistance.



348

349 **References**

350 Ahn J, Brook EJ (2008) Atmospheric CO₂ and climate on millennial time scales during the last
351 glacial period. *Science*, 322 (5898), 83-85.

352 Allen JRM, Brandt U, Brauer A et al (1999) Rapid environmental changes in southern Europe
353 during the last glacial period. *Nature* 400, 740-743.

354 Andersen KK, Azuma N, Barnola JM et al (2004) High-resolution record of Northern Hemisphere
355 climate extending into the last interglacial period. *Nature*, 431 (7005), 147-151.

356 Aranbarri J, González-Sampériz P, Valero-Garcés B, Moreno A, Gil-Romera G, Sevilla-Callejo M,
357 García-Prieto E, Di Rita M., Mata P, Morellón M, Magri D, Rodríguez-Lázaro J, Carrión JS
358 (2014). Rapid climatic changes and resilient vegetation during the Lateglacial and Holocene in a
359 continental region of south-western Europe. *Global and Planetary Change*, 114, 50-65.

360 Augustin L, Barbante C, Barnes PR et al (2004) Eight glacial cycles from an Antarctic ice core.
361 *Nature*, 429 (6992), 623-628.

362 Behling H, Safford HD (2010) Late-glacial and Holocene vegetation, climate and fire dynamics in
363 the Serra dos Órgãos, Rio de Janeiro State, southeastern Brazil. *Global Change Biology*, 16
364 (6), 1661-1671.

365 Bird M, Cali J (1998) A million-year record of fire in sub-Saharan Africa. *Nature*, 394 (6695),
366 767-769.

367 Blunier T, Brook EJ (2001) Timing of millennial-scale climate change in Antarctica and
368 Greenland during the last glacial period. *Science*, 291 (5501), 109-112.

369 Bond G, Showers W, Cheseby M et al (1997) A pervasive millennial-scale cycle in North Atlantic
370 Holocene and glacial climates. *Science* 278, 1257-1266.

371 Bowman DM, Balch JK, Artaxo P et al (2009) Fire in the Earth system. *science*, 324 (5926),
372 481-484.

373 Callaway E (2015) Teeth from China reveal early human trek out of Africa-"Stunning" find shows
374 that *Homo sapiens* reached Asia around 100,000 years ago. *Nature News*,
375 (www.nature.com/news/teeth-from-china-reveal-early-human-trek-out-of-africa-1.18566)

376 Chen FH, Bloemendal J, Wang JM, Li JJ, Oldfield F (1997) High-resolution multiproxy climate
377 records from Chinese loess: evidence for rapid climatic changes over the last 75 ka.



- 378 Palaeogeography, Palaeoclimatology, Palaeoecology 130, 323-335.
- 379 Cheng H, Edwards RL, Sinha A et al (2016) The Asian monsoon over the past 640,000 years and
380 ice age terminations. *Nature*, 534 (7609), 640-646.
- 381 Cheng H, Zhang PZ, Spöhl C et al (2012) The climatic cyclicity in semiarid - arid central Asia
382 over the past 500,000 years. *Geophysical Research Letters*, 39 (1), L0170510.
- 383 Conard NJ, Bolus M (2008). Radiocarbon dating the late Middle Paleolithic and the Aurignacian
- 384 Crawford AJ, Belcher CM (2014) Charcoal morphometry for paleoecological analysis: The effects
385 of fuel type and transportation on morphological parameters. *Applications in plant sciences*,
386 2, 8.
- 387 Dennell RW, Rendell HM, Hailwood E (1988) Late Pliocene Artefacts from Northern Pakistan.
388 *Current Anthropology*, 29, 3, 495-498.
- 389 Filion L (1984) A relationship between dunes, fire and climate recorded in the Holocene deposits
390 of Quebec. *Nature*, 543-546.
- 391 Foley R, Gamble C (2009) The ecology of social transitions in human evolution. *Philos Trans R*
392 *Soc Lond B Biol Sci.*, 364 (1533), 3267-3279.
- 393 Fu Q, Meyer M, Gao X et al (2013) DNA analysis of an early modern human from Tianyuan Cave,
394 China. *Proceedings of the National Academy of Sciences*, 110 (6), 2223-2227.
- 395 Gao X (2014) Archaeological evidence for Evolutionary continuity of Pleistocene humans in
396 China and east Asia and related discussions. *Acta Anthropol Sin*, 33, 237-253.
- 397 Glasspool IJ, Edwards D, Axe L (2004) Charcoal in the Silurian as evidence for the earliest
398 wildfire. *Geology*, 32 (5), 381-383.
- 399 Goren-Inbar N, Alperson N, Kislev ME et al (2004) Evidence of hominin control of fire at Gesher
400 Benot Yaaqov, Israel. *Science*, 304 (5671), 725-727.
- 401 Guiot J, De Beaulieu JL, Cheddadi R et al (1993) The climate in Western Europe during the last
402 Glacial/Interglacial cycle derived from pollen and insect remains. *Palaeogeography,*
403 *Palaeoclimatology, Palaeoecology* 103 (1), 73-93.
- 404 Guo ZT, Liu TS, Guiot J et al (1996) High frequency pulses of East Asian monsoon climate in the
405 last two glaciations: link with the North Atlantic. *Climate Dynamics*, 12 (10), 701-709.
- 406 Han WX, Lu LP, Lai Z, Madsen D, Yang SL (2014) The earliest well-dated archeological site in
407 the hyper-arid Tarim Basin and its implications for prehistoric human migration and climatic



- 408 change. *Quaternary Research*, 82 (1), 66-72.
- 409 Hao Q, Wang L, Oldfield F et al (2012) Delayed build-up of Arctic ice sheets during 400,000-year
410 minima in insolation variability. *Nature*, 490, 7420, 393-396.
- 411 Huang CC, Pang J, Chen S et al (2006) Charcoal records of fire history in the Holocene loess-soil
412 sequences over the southern Loess Plateau of China. *Palaeogeography, Palaeoclimatology,*
413 *Palaeoecology*, 239, 1, 28-44.
- 414 Huang WW, Olsen JW, Reeves RW, Miller-Antonio S, Lei JQ (1988) New discoveries of stone
415 artifacts on the southern edge of the Tarim Basin, Xinjiang. *Acta Anthropologica Sinica* 4,
416 294-301 (in Chinese).
- 417 Hubau W, Van den Bulcke J, Van Acker J, Beeckman H (2015) Charcoal-inferred Holocene fire
418 and vegetation history linked to drought periods in the Democratic Republic of Congo.
419 *Global change biology*, 21(6), 2296-2308.
- 420 Hublin JJ (2012) The earliest modern human colonization of Europe. *Proc Natl Acad Sci USA* 109(34),
421 13471–13472.
- 422 Jiang HC, Mao X, Xu H, Thompson J, Wang P, Ma X (2011) Last glacial pollen record from
423 Lanzhou (Northwestern China) and possible forcing mechanisms for the MIS 3 climate
424 change in Middle to East Asia. *Quaternary Science Reviews*, 30 (5), 769-781.
- 425 Klein RG (2008) Out of Africa and the evolution of human behavior. *Evol Anthropol* 17(6), 267–281.
- 426 Krause J, Fu Q, Good JM, Viola B, Shunkov MV, Derevianko AP, Pääbo S (2010). The complete
427 mitochondrial DNA genome of an unknown hominin from southern Siberia. *Nature*, 464
428 (7290), 894-897.
- 429 Li F, Kuhn SL, Gao X, Chen FY (2013) Re-examination of the dates of large blade technology in
430 China: A comparison of Shuidonggou Locality 1 and Locality 2. *Journal of Human Evolution*,
431 64,161-168.
- 432 Li XZ, Liu XD, Qiu LJ, An ZS, Yin ZY (2013) Transient Simulation of Orbital-scale Precipitation
433 Variation in Monsoonal East Asia and Arid Central Asia during the Last 150 ka. *J. Geophys.*
434 *Res.*, 118, 7481-7488.
- 435 Li Y, Song Y, Lai Z, Han L, An Z (2016) Rapid and cyclic dust accumulation during MIS 2 in
436 Central Asia inferred from loess OSL dating and grain-size analysis. *Scientific Reports*, 6,
437 e32365:32361-32366.



- 438 Li Y, Song YG, Yan LB, Chen T, An ZS (2015) Timing and Spatial Distribution of Loess in
439 Xinjiang, NW China. *Plos One*, 10, 5.
- 440 Liu W, Martín-Torres M, Cai YJ et al (2015) The earliest unequivocally modern humans in
441 southern China. *Nature* doi:10.1038/nature15696
- 442 Lu HY, Xia XC, Liu JQ et al (2010) A preliminary study of chronology for a newly discovered
443 ancient city and five archaeological sites in Lop Nur, China. *Chin Sci Bull* 55 (1), 63-71 (in
444 Chinese).
- 445 Luo Y, Chen H, Wu G, Sun X (2001) Records of natural fire and climate history during the last
446 three glacial-interglacial cycles around the South China Sea. *Science in China Series D:
447 Earth Sciences*, 44, 10, 897-904.
- 448 Mellars P (2006) Archeology and the dispersal of modern humans in Europe: Deconstructing the
449 “Aurignacian”. *Evol Anthropol* 15(5), 167–182.
- 450 Mellars P (2006) Going east: new genetic and archaeological perspectives on the modern human
451 colonization of Eurasia. *Science*, 313, 5788, 796-800.
- 452 Miao YF, Jin H, Cui J (2016a), Human activity accelerating the rapid desertification of the Mu Us
453 Sandy Lands, North China. *Scientific reports*, 6.
- 454 Miao YF, Zhang D, Cai X et al (2016b) Holocene fire on the northeast Tibetan Plateau in relation
455 to climate change and human activity. *Quaternary International*.
- 456 Nigst P R, Haesaerts P, Damblon F, et al. (2014). Early modern human settlement of Europe north of
457 the Alps occurred 43,500 years ago in a cold steppe-type environment. *Proceedings of the
458 National Academy of Sciences* 111(40), 14394-14399.
- 459 of the Swabian Jura. *J. Hum. Evol.* 55 (5), 886–897.
- 460 Patterson WA, Edwards KJ, Maguire DJ (1987) Microscopic charcoal as a fossil indicator of fire.
461 *Quaternary Science Reviews*, 6 (1), 3-23.
- 462 Petit JR, Jouzel J, Raynaud D et al (1999) Climate and atmospheric history of the past 420,000
463 years from the Vostok ice core, Antarctica. *Nature*, 399 (6735), 429-436.
- 464 Porter SC, An ZS (1995) Correlation between climate events in the North Atlantic and China
465 during the last glaciation. *Nature* 375, 305- 308.
- 466 Rao ZG, Chen FH, Cheng H et al (2013) High-resolution summer precipitation variations in the
467 western Chinese Loess Plateau during the last glacial. *Scientific reports*, 3, 2785.



- 468 Shen CD, Yi WX, Yang Y et al (2004) Concentrations of elemental carbon in samples from the
469 Peking Man Site at Zhoukoudian and the possibility of their application in the development
470 of evidence for the use of fire by humans. *Chinese Science Bulletin*, 49 (6), 612-616.
- 471 Sirocko F, Knapp H, Dreher F, Förster MW, Albert J, Brunck H, Röhner M, Rudert S, Schwibus K,
472 Adams C, Sigl P (2016). The ELSA-Vegetation-Stack: Reconstruction of Landscape Evolution
473 Zones (LEZ) from laminated Eifel maar sediments of the last 60,000 years. *Global and Planetary
474 Change*, 142, 108-135.
- 475 Song YG, Chen XL, Qian LB et al (2014) Distribution and composition of loess sediments in the
476 Ili Basin, Central Asia. *Quaternary International* 334-335, 61-73.
- 477 Song YG, Chen XL, Qian LB et al (2014) Distribution and composition of loess sediments in the
478 Ili Basin, Central Asia. *Quat Int* 334-335, 61-73.
- 479 Song YG, Lai ZP, Li Y et al (2015) Comparison between luminescence and radiocarbon dating of
480 late Quaternary loess from the Ili Basin in Central Asia. *Quaternary Geochronology*, 30,
481 405-410.
- 482 Song YG, Li CX, Zhao JD, Chen P, Zeng M (2012) A combined luminescence and radiocarbon
483 dating study of the Ili loess, Central Asia. *Quaternary Geochronology* 10, 2-7.
- 484 Song YG, Shi ZT, Fang XM et al (2010) Loess magnetic properties in the Ili Basin and their
485 correlation with the Chinese Loess Plateau. *Science China Earth Sciences* 53, 419-431.
- 486 Sun YB, Clemens SC, Morrill C et al (2012) Influence of Atlantic meridional overturning
487 circulation on the East Asian winter monsoon. *Nature Geosci*, 5 (1), 46-49.
- 488 Taklimakan Desert archaeology group (1990) Microlithic in the AltunMountains. *Xinjiang
489 Cultural Relics* 4, 14-18 (in Chinese)
- 490 Tang ZH, Chen D, Wu X, Mu G. (2013) Redistribution of prehistoric Tarim people in response to
491 climate change. *Quat Int* 308, 36-41.
- 492 Templeton A (2002) Out of Africa again and again. *Nature*, 416 (6876), 45-51.
- 493 Thompson L, Yao TD, Davis M et al (1997) Tropical climate instability: The last glacial cycle
494 from a Qinghai-Tibetan ice core. *Science*, 276 (5320), 1821-1825.
- 495 Trinkaus E, Moldovan O, Bilgär A, et al. (2003). An early modern human from the Peștera cu Oase,
496 Romania. *Proc Natl Acad Sci USA* 100 (20), 11231–11236.
- 497 Umbanhowar CE, Mcgrath MJ (1998) Experimental production and analysis of microscopic



- 498 charcoal from wood, leaves and grasses. *The Holocene*, 8 (3), 341-346.
- 499 Varela S, Lima-Ribeiro MS, Diniz-Filho JAF, Storch D (2015) Differential effects of temperature
500 change and human impact on European Late Quaternary mammalian extinctions. *Global*
501 *change biology*, 21 (4), 1475-1481.
- 502 Wang B, Zhang TN (1988) New discoveries of the Paleolithic archaeology in Xinjiang. *Social*
503 *Science Research of Xinjiang* 11, 35-36 (in Chinese).
- 504 Wang QS., Song YG, Zhao ZJ, Li JJ (2016) Color characteristics of Chinese loess and its
505 paleoclimatic significance during the last glacial-interglacial cycle. *J Asian Earth Sci* 116,
506 132-138.
- 507 Wang X, Xiao J, Cui L, Ding ZL (2013) Holocene changes in fire frequency in the Daihai Lake
508 region (north-central China): indications and implications for an important role of human
509 activity. *Quaternary Science Reviews*, 59, 18-29.
- 510 Wang Y, Cheng H, Edwards RL et al (2008) Millennial- and orbital-scale changes in the East
511 Asian monsoon over the past 224,000 years. *Nature*, 451 (7182), 1090-1093.
- 512 Weiner S, Xu Q, Goldberg P, Liu J, Bar-Yosef O (1998) Evidence for the use of fire at
513 Zhoukoudian, China. *Science*, 281, 251-253.
- 514 Whitlock C, Larsen C (2002) Charcoal as a fire proxy, *Tracking environmental change using lake*
515 *sediments*, Springer, 75-97.
- 516 Yang SL, Forman SL, Song YG et al (2014) Evaluating OSL-SAR protocols for dating quartz
517 grains from the loess in Ili Basin, Central Asia. *Quat Geoch* 20, 78-88.
- 518 Yidilis A (1993) Microlithic sites in Xinjiang. *Xinjiang Cultural Relics* 4, 17-18 (in Chinese).
- 519 Zhang F, Wang T, Yimit H et al (2011) Hydrological changes and settlement migrations in the
520 Keriya River delta in central Tarim Basin ca. 2.7-1.6 ka BP: inferred from ^{14}C and OSL
521 chronology. *Sci China Earth Sci* 41, 1495-1504 (in Chinese).
- 522 Zhao Y, Chen F, Zhou A, Yu Z, Zhang K (2010) Vegetation history, climate change and human
523 activities over the last 6200 years on the Liupan Mountains in the southwestern Loess Plateau
524 in central China. *Palaeogeography, Palaeoclimatology, Palaeoecology*, 293 (1), 197-205.
- 525